HHS Public Access

Author manuscript

Wound Repair Regen. Author manuscript; available in PMC 2020 May 31.

Published in final edited form as:

Wound Repair Regen. 2019 March ; 27(2): 139–149. doi:10.1111/wrr.12691.

Plasma-based biomaterials for the treatment of cutaneous radiation injury

Eric D. Miller, MD, PhD[1], **Feifei Song, MS**[1], **Jason D. Smith, PhD**[2,3], **Ahmet S. Ayan, PhD**[1], **Xiaokui Mo, PhD**[4], **Michael Weldon, MS**[1], **Lanchun Lu, PhD**[1], **Phil G. Campbell, PhD**[2], **Aashish D. Bhatt, MD**[1], **Arnab Chakravarti, MD**[1], **Naduparambil K. Jacob, PhD**[1]

[1]Department of Radiation Oncology, Comprehensive Cancer Center, The Ohio State University, Columbus, Ohio,

[2]Engineering Research Accelerator, Carnegie Mellon University, Pittsburgh, Pennsylvania,

[3]Carmell Therapeutics, Pittsburgh, Pennsylvania

[4]Center for Biostatistics, The Ohio State University, Columbus, Ohio

Abstract

Cutaneous wounds caused by an exposure to high doses of ionizing radiation remain a therapeutic challenge. While new experimental strategies for treatment are being developed, there are currently no off-the-shelf therapies for the treatment of cutaneous radiation injury that have been proven to promote repair of the damaged tissues. Plasma-based biomaterials are biologically active biomaterials made from platelet enriched plasma, which can be made into both solid and semi-solid forms, are inexpensive, and are available as off-the-shelf, nonrefrigerated products. In this study, the use of plasma-based biomaterials for the mitigation of acute and late toxicity for cutaneous radiation injury was investigated using a mouse model. A 2-cm diameter circle of the dorsal skin was irradiated with a single dose of 35 Gy followed by topical treatment with plasma-based biomaterial or vehicle once daily for 5 weeks postirradiation. Weekly imaging demonstrated more complete wound resolution in the plasma-based biomaterial vs. vehicle group which became statistically significant ($p < 0.05$) at weeks 12, 13, and 14 postmaximum wound area. Despite more complete wound healing, at 9 and 17 weeks postirradiation, there was no statistically significant difference in collagen deposition or skin thickness between the plasma-based biomaterial and vehicle groups based on Masson trichrome staining nor was there a statistically significant difference in inflammatory or fibrosis-related gene expression between the groups. Although significant improvement was not observed for late toxicity, plasma-based biomaterials were effective at promoting wound closure, thus helping to mitigate acute toxicity.

Reprint requests: Naduparambil Jacob, PhD, Department of Radiation Oncology, The James Cancer Hospital and Solove Research Institute, Ohio State University Wexner Medical Center, 400 W. 12th Ave., Columbus, OH 43210. Tel: +614 685-4246; Fax: +1614 688-4994; naduparambil.jacob@osumc.edu.

Conflicts of Interest: Jason Smith, PhD, was an employee of Carmell Therapeutics while this study was being conducted, but did not perform the experiments or perform primary analysis of the data. This study was not funded by Carmell Therapeutics.

Cutaneous radiation injury (CRI) following accidental or intentional acute exposure to large doses of ionizing radiation is a challenging medical problem.[1] Radiation-induced wounds appear as a delayed effect following exposure.[2] They can be extremely painful, life-threatening due to risk of infection, and heal slowly with the possibility of incomplete healing and recurrence.[2] With terrorism occurring on a global scale, the threat of a large-scale radiologic attack remains imminent.[3] Consequently, the development of mitigating agents against the acute and late toxicities of radiation exposure remains a high priority. Radiation is also used as a primary or adjuvant therapy for many types of cancer. Radiation dermatitis remains a significant challenge in patients being treated for disease sites such as the head and neck which may result in secondary infections, hospital admissions, and treatment breaks which may result in inferior local control of the disease.[4] With efforts focused on radiation dose escalation,[5] the increasing use of re-irradiation for some cancers,[6] and the more widespread use of protons which do not necessarily spare the skin,[7] radiation dermatitis will continue to be a significant issue in the management of cancer patients receiving radiation therapy.[8]

Currently, there are no off-the-shelf therapies available for the treatment of CRI that have been proven to promote repair of the damaged tissues. Plasma-based biomaterials (PBMs) are biologically active biomaterials made from platelet enriched plasma, which contains a concentration of growth factors that naturally stimulate wound repair.[9] PBMs can be manufactured in a variety of forms, including flexible sheets, powders, pastes, and putties, and their biodegradation rates can be tuned for controlled release of bioactivity spanning weeks to months. They are inexpensive, safe, and available as off-the-shelf products that do not require refrigeration. Manufacturing PBMs using pooled plasma units from US blood banks which have already undergone rigorous viral screening offers an extremely low risk of viral transmission. However, an additional proprietary viral inactivation process is used during the PBM manufacturing process as an additional safety precaution. They are made from pooled human plasma units (from US blood banks), which allows for lot-to-lot consistency, product characterization, and viral screening. Viral inactivation methods, however, are used during manufacturing as an additional safety precaution. The PBM manufacturing process retains the biological activity of the blood plasma, which means that the biomaterial will release natural blood plasma-derived growth factors (e.g., insulin-like growth factor [IGF-1], platelet-derived growth factor (PDGF), and vascular endothelial growth factor) into the tissue site. Additionally, there is potential evidence to suggest that PBMs stimulate the body to naturally fight infection.[10] While PBMs contain the same growth factors as autologous platelet-rich plasma (PRP) therapies, which have been used in a variety of applications to augment wound healing, including promotion of wound healing following irradiation in porcine models,[11] PBMs overcome many of the limitations of PRP therapies. In particular, current PRP therapies: (1) have inherent variability due to patient-to-patient differences in platelet counts and growth factors as well as clinic-to-clinic differences in preparation protocols; (2) poor localization at the site of injury as PRP is delivered in liquid form and has a relatively short residence time; and, (3) are not off-the-shelf. PBMs were specifically designed to overcome these critical limitations of PRP. PBMs have been used to deliver antibiotics to reduce the incidence of pacemaker pocket infections using a rabbit model[10] and have been impregnated with amiodarone to reduce the risk of atrial

fibrillation in a post-cardiac surgery porcine model.[12] In addition, PBMs have been shown to stimulate cell proliferation in vitro and used to stimulate the repair of a bone defect using a mouse calvarial defect model.[9] A first-in-man clinical trial of a putty form of PBM for the repair of open tibia fractures was recently completed in South Africa. Even with a small patient population, the study demonstrated that treatment with PBM (20 patients; standard fixation plus putty) improved bone healing at 6 months, demonstrating statistically significant fewer infections compared to the control group and trending for accelerated soft tissue healing around the tibia (10 patients; standard fixation; manuscript in preparation). These data indicate the efficacy of PBMs for soft tissue healing as well as infection reduction, which are both directly applicable to wound healing.

Due to the favorable properties of the PBMs for stimulating tissue repair and fighting infection, we have conducted this study to evaluate the use of PBM-based topical agents for the treatment of CRI. Our hypothesis was that PBM-based topical therapies delivered within 24 hours after an acute localized high-dose radiation exposure in mice may result in accelerated resolution of cutaneous injury when compared to vehicle control. Furthermore, by promoting healing of the damaged tissue, topical PBM may mitigate late toxicity following radiation exposure including chronic/delayed ulcer formation and fibrosis.

MATERIALS AND METHODS

PBM paste

Plasma powder was prepared by first pooling multiple units of virus screened, frozen human plasma (with platelets) obtained from the Central Blood Bank (Pittsburgh, PA). The pooled plasma was clotted by adding calcium chloride to 18 mM final concentration to activate the endogenous thrombin. The clotted plasma was then freeze-dried and ground into a powder. Two proprietary viral inactivation methods were used during these plasma processing steps to inactivate any potential viruses contained within the plasma.[9]

PBMs were made by mixing plasma powder and glycerol into a dough, which was then processed using proprietary manufacturing processes to bind and crosslink the plasma powder into a biomaterial. The solid biomaterial was then ground into particles, and the particle form of the PBM was mixed with Aquaphor (Beiersdorf AG, Hamburg, Germany) at 10% PBM by weight to create a PBM paste in Aquaphor base. The pastes were packaged into jars and stored at room temperature. Biocompatibility and bioactivity of PBM as well as growth factor composition has been confirmed in a prior study.[9]

In vivo model

Prior to experiments, the protocol was approved by the Institutional Animal Care and Use Committee of The Ohio State University (Protocol number 2011A00000029). Animal experiments complied with those set forth by the National Institutes of Health guide for the care and use of laboratory animals. Male *Mus musculus* strain BALB/c between 9 and 11 weeks old were used for all experiments. All animals were fed a regular rodent diet and provided water ad libitum. The day prior to irradiation, the mice were anesthetized with an intraperitoneal injection of 100 mg/kg ketamine hydrochloride (JHP Pharmaceuticals, LLC)

and 10 mg/kg xylazine hydrochloride (Sigma-Aldrich, St. Louis, MO) diluted in sterile phosphate-buffered saline and the backs of the mice were shaved with electric clippers being careful not to nick the skin. On the day of irradiation, the mice were again anesthetized using an intraperitoneal injection of the same concentration of ketamine/xylazine and placed in a custom acrylic holder with a 2 mm thick lead cover. The dorsal skin of each mouse was pulled through a slit in the lead cover and taped to the surface of the lead shielding with the rest of the body protected from radiation as shown in Figure 1A. A 2-cm diameter circle of skin was exposed to a single dose of 35 Gy using an RS 2000 biological irradiator (Rad Source Technologies, Suwanee, GA) with 165 kV x-rays. Prior to irradiation, dosimetry was performed using nanoDot optically stimulated luminescent detectors (Landauer, Glenwood, IL) to verify the delivered dose to the skin.[13] Following irradiation, the area of exposed skin was marked using a permanent marker and the mice were allowed to recover from anesthesia.

Topical treatment was initiated within 24 hours following radiation exposure. Group 1 (n = 22) was treated with Aquaphor alone (will be referred to as vehicle) while group 2 (n = 22) was treated with Aquaphor/PBM (will be referred to as PBM). For each treatment, the mice were anesthetized with isoflurane delivered by facemask and 0.3 ml of either the vehicle or PBM was measured using a 0.1 ml sample spoon (Grainger, Lake Forest, IL), and spread topically in a thin film on the irradiated area. The area was then covered with bandages as shown in Figure 1B. Treatments were administered for 5 days per week for a total of 5 weeks post-irradiation. Five animals from both the PBM group and vehicle group were lost secondary to anesthesia deaths during the course of the entire experiment.

Image acquisition and analysis

Images of the mice were acquired weekly using a custom imaging system that allowed reproducible image acquisition with uniform lighting using paired 5,600 K LED light sources (Neewer, Guangdong, China) at a fixed magnification. During each image acquisition, mice were anesthetized with isoflurane delivered via facemask and digital images of the backs of the mice were acquired using a Sony Cybershot WX350 digital camera (Sony Corporation, Minato, Tokyo, Japan). To minimize the subjectivity of visual scoring, the wound area was evaluated using automated image analysis using MATLAB software pack-age.[14] A 2 × 5 cm piece of Delrin (DuPont, Wilmington, DE) was placed in each image field as a white standard. After white balance correction using the white standard, segmentation was based on color and performed in CIE $L^*a^*b^*$ color space using a k-means clustering algorithm.[15] For the test images, color clusters determined by the k-means algorithm were compared against the human observer's color-based segmentation. The range of values for the a^* and the b^* parameters in CIELab color space for the color cluster that most closely matched the human observer's segmentation were taken as the threshold range and this threshold range was then applied to all images for automatic segmentation. The wound area was then converted from pixels to square millimeters using a conversion factor derived using a graticule of known size. An example of an acquired image and the same image following automated segmentation is shown in Figure 1C and D, respectively.

Histology

The mice were euthanized and cutaneous tissue from the irradiated area was harvested at weeks 9 and 17 post-irradiation. The circular piece of irradiated tissue was cut in half with the anterior half used for histology and the posterior half used for gene expression analysis (see Gene Expression below). Control skin which was not irradiated or treated with vehicle or PBM was harvested from the abdomen of the mice. After harvesting, the skin was placed on an index card, fixed in 10% neutral-buffered formalin, and processed for hematoxylin and eosin (H&E) and Masson's trichrome staining using standard histological techniques. Both the H&E and Masson's trichrome stained slides were then digitally captured using a Scanscope XT scanner (Leica, Wetzlar, Germany). To measure collagen deposition, measurements of skin thickness in the irradiated area were performed. Images of the trichrome-stained slides were processed using ImageJ (v1.49v, National Institutes of Health, Bethesda, MD). Each tissue section was divided into 10 equal sections and measurements of the four central sections were obtained to exclude edge artifacts from histologic processing. The measurements were performed at 4x magnification and included from the dermal-subcutaneous interface to the external surface of the epidermis.

Gene expression (NanoString gene expression analysis)

The posterior portion of the skin that was removed at the week 17 postirradiation time point was utilized for RNA isolation ($n = 5$ mice) to evaluate gene expression involved in inflammation and fibrosis. At time of harvest, the central irradiated area of dorsal skin was dissected into submillimeter sections, flash-frozen in liquid nitrogen, and stored at −80 °C. RNA was extracted from the tissue using the mirVana miRNA Isolation Kit (Thermo Fisher Scientific, Waltham, MA) and quantitated by the NanoDrop 2000 Spectrophotometer (Thermo Fisher Scientific). RNA quality was estimated by the Agilent RNA 6000 Nano Assay (Agilent Technologies, Santa Clara, CA). RNA was subjected to the NanoString nCounter gene expression assay (XT-CSO-MIP1-12; NanoString Technologies, Seattle, WA) as completed by Genomics Shared Resource-Comprehensive Cancer Center according to the manufacturer's protocol. Raw data were analyzed by nSolver software (NanoString Technologies) using standard settings and were normalized against the housekeeping genes (Abcf1, Hprt, and Oaz1) and fold changes of selected genes involved in inflammation and fibrosis were calculated.

Statistical analysis

SAS statistical software (SAS Institute, Cary, NC) was used for all data analysis. The association between treatment groups and the probability of chronic wound formation was analyzed using Fisher's exact test. For the wound area analysis, the mean wound area for the mice at each time point was normalized by log2 transformation of the data. The ratio of mean wound area between treatment and vehicle at each time point was tested using a mixed-effects model incorporating repeated measures for each mouse. For the skin thickness measurements, the mean thickness based on the four central measured sections was obtained for each treatment group as well as the control area for each mouse. Data were then analyzed using ANOVA followed by pairwise comparisons. Quantitative data is presented as means

standard error of mean unless otherwise noted. Statistical significance was defined as $p < 0.05$.

RESULTS

Wound healing based on image analysis

Representative images from the control and experimental groups over time are shown in Figure 2. Maximum injury was observed around 3–4 weeks postirradiation with erythema, moist desquamation, and ulceration present in both groups with a similar wound size observed in the PBM 242.7 ± 37.5 mm^2 and vehicle 216.4 ± 50.4 mm^2 groups, $p = 0.08$. Initial resolution of the injury in both groups was apparent at 6 weeks postirradiation including substantial hair regrowth. At 12 weeks postirradiation, recurrent ulceration was observed more often in the vehicle group. By 17 weeks postirradiation, which was the final time-point of the experiment, the wound area of the vehicle group was very similar to the 12 week postirradiation time-point indicating recurrent ulceration. In the PBM group, either a decrease in size of the wound area or complete resolution of the wound was observed. However, there were mice in the PBM group that developed nonhealing wounds as well, as observed in the second row of the figure. Overall, large chronic nonhealing wounds were more often observed in the vehicle group (5/7 mice, 71%) compared to the PBM group (2/7 mice, 29%) at the 10–14 week postirradiation time points although this did not reach statistical significance, $p = 0.29$.

A graph of wound area over time for the mice in the PBM and vehicle groups ($n = 22$ mice in each group at the start of the experiment) is shown in Figure 3. In this graph, the wound area is expressed as a percentage of the maximum wound area which was observed 3 to 4 weeks postirradiation. Therefore, week 1 on the graph represents either week 4 or 5 after irradiation. As seen in the graph, the wound area closure over time between the two groups was similar until 10 weeks postmaximum wound area at which point a separation between the two groups was observed. The difference between the groups became subsequently larger over time and at weeks 12, 13, and 14, a statistically significant difference between the two groups was observed. At 12 weeks postmaximum wound area, the PBM group wound area was 14.1 ± 5.2% (mean SEM) while the vehicle group wound area was 34.3 ± 6.1%, $p < 0.05$. At 13 weeks postmaximum wound area, the PBM group wound area was 12.1 ± 3.9% and the vehicle group was 29.2 ± 7.0%, $p < 0.05$. Finally, at 14 weeks postmaximum wound area, the PBM group wound area was 5.7 ± 3.7% and the vehicle wound area was 20.7 ± 8.2%, $p < 0.05$.

Histologic analysis and skin thickness measurements

Mice were sacrificed at weeks 9 and 17 postirradiation and the irradiated and control skin (from the abdomen) was harvested for histologic analysis. Representative images of H&E stains from the 9 week postirradiation time period are shown in Figure 4. When comparing the PBM to vehicle alone group, epidermal hyperplasia, hyperkeratosis, and inflammatory cell infiltrate was present and apparent in both groups when compared with the control skin which was not irradiated or treated. However, as reflected in the wound healing measurements, the area of skin where these histological changes were present was generally

smaller in the PBM compared to the vehicle alone group. Representative images from the 17 week postirradiation time point are shown in Figure 5. In the representative example shown, a continued degree of epidermal hyperplasia was present in the skin treated with PBM (Figure 5A and D), which was less severe than that observed in the vehicle alone group (Figure 5B and E). In addition, hyperkeratosis persisted in the vehicle alone group.

To evaluate the extent of fibrosis, Masson's trichrome staining was performed on samples from each of the time points and the skin thickness was measured from the dermal-subcutaneous interface to the external surface of the epidermis. Representative images are shown in Figure 6A–C and E–G with a summary of the measurements shown in Figure 6D and H. For the 9 week postirradiation time point, the skin thickness for the PBM-treated group was 417 ± 64 μm (mean SEM), for the vehicle group was 434 ± 94 μm, and for the control group was 303 ± 26 μm. While the measured skin in the vehicle group was thicker than the PBM group, the difference did not reach statistical significance ($p = 0.86$). Likewise, both the PBM and vehicle group skin measurements were thicker than the control group, but this difference did not reach statistical significance, $p = 0.22$ and $p = 0.16$, respectively. At 17 weeks postirradiation, the skin in the vehicle group remained thicker than that of the PBM group, 544 ± 86 vs. 468 ± 86 μm, but again did not reach statistical significance with $p = 0.47$. Both the PBM and vehicle groups had skin measurements that were thicker than the control group which was 327 22 μm. The difference in thickness between the PBM and control groups was not statistically significant ($p = 0.21$) while there was a trend for significance between the vehicle and control groups ($p = 0.06$).

Gene expression analysis

As there was no statistically significant difference in skin thickness observed histologically between the PBM and vehicle groups at the 17 week postirradiation time point, gene expression analysis was performed to evaluate for differential expression of fibrosis and chronic inflammatory genes. This analysis revealed no statistically significant difference between the vehicle and PBM groups in expression of inflammatory genes including Il1a, Il1b, and Il1rn as shown in Figure 7A–C. Similarly, there was no statistically significant difference observed in fibrosis gene expression in the irradiated skin between the vehicle and PBM groups including Tgfb1, Spp1, and Stat3 as shown in Figure 7D–F.

DISCUSSION

Skin is a relatively radiosensitive organ due to the presence of rapidly proliferating and maturing cells.[8] The degree of skin damage following a localized radiation exposure is dose-dependent with temporary epilation occurring at 3–5 Gy, erythema at 5–6 Gy, and more severe damage occurring above 10 Gy progressing from desquamation to ulceration to necrosis with increasing dose.[2] Radiation exposure causes a disruption in the normal sequence of events in wound healing.[16] The early effects of radiation exposure result in an increase in vascular permeability due to endothelial cell apoptosis and an increase in the synthesis of pro-inflammatory cytokines including tumor necrosis factor-α, interferon-γ, and interleukin-1 and interleukin-8.[16–18] The inflammatory response is prolonged following an exposure due to an overabundance of pro-inflammatory signaling molecules resulting in

defective collagen deposition.[17] The long-term effect of the initial endothelial cell damage after acute radiation exposure is ischemic damage.[17] Fibroblasts are also attracted to the injured site following exposure which results in increased accumulation of extracellular matrix components at the wound site and subsequent radiation fibrosis largely driven by transforming growth factor β1 (TGF-β1).[17,19] Radiation toxicity is typically classified into acute toxicity occurring hours to weeks following exposure and late toxicity which may present months to years following exposure. Acute cutaneous toxicity may result in erythema, edema, hyperpigmentation, depilation, and desquamation while chronic cutaneous toxicity may manifest as fibrosis, permanent hyperpigmentation, telangi-ectasias, atrophy, and delayed/persistent ulceration.[8,20]

While a standardized approach for the treatment of severe CRI does not exist,[21] the mainstay is surgical excision and either skin grafting or flap placement.[22] However, healing outcomes remain uncertain. New lesions can appear weeks, months, or even years later, requiring excision with additional reconstruction, with many extremity cases ultimately ending in amputation.[23,24] Cell-based therapies have been investigated with the focus primarily on mesenchymal stem cells. Francois et al. injected human mesenchymal stem cells (hMSCs) into the tail vein of immunodeficient mice 24 hours after exposing the right hind leg to 30 Gy with a ^{60}Co source.[25] The mice treated with hMSCs developed a less severe injury following radiation exposure than the untreated group as well as improved healing. Horton et al. evaluated the use of bone marrow-derived mesenchymal stem cells (MSCs) delivered systemically on cutaneous radiation-induced fibrosis following exposure of the right hind leg of a mouse to 35 Gy.[26] The treated mice were found to have reduced skin thickening and collagen deposition when compared to the untreated mice. A promising new treatment for severe CRI is the use of dosimetry-guided surgery combined with delivery of autologous MSCs.[1,23,25] This technique has been used in several case reports to treat patients following large incidental cutaneous radiation exposures with excellent results.[1,23] The main limitations of this approach are the availability of MSCs and the cost associated with obtaining and expanding the cells in the event of a large-scale incident. Growth factors have also been shown to have wound healing activity in irradiated tissue. Following cutaneous radiation exposure, topical recombinant human PDGF-BB has been shown to accelerate wound healing[27] while topical recombinant human epidermal growth factor has been shown to reduce the risk of recurrent radiation dermatitis.[28] However, the limitations of growth factor therapy include expense, a limited shelf life, and limited availability.[29] Reisman et al. reported on the use of topical RTA 408, which is a synthetic triterpenoid with antioxidant and anti-inflammatory properties, to prevent radiation dermatitis using a mouse model treated with fractionated external beam radiation.[30] A dose-dependent improvement in the appearance of the skin both grossly and histologically was noted with increasing concentrations of topical RTA 408.

An increasing number of studies are being performed to investigate the utility of blood plasma-based products for the treatment of radiation induced tissue injury. Osteoradionecrosis of the mandible is a serious complication of head and neck radiation therapy resulting in pain, possible infection, and even pathologic fracture.[31] Currently, the optimal way to manage osteoradionecrosis is unknown.[31] Several case reports and large patient series documenting the use of PRP for the effective treatment of osteoradionecrosis

have been published.[32–34] A limited number of prospective studies using PRP have been performed with mixed results. Most of these studies use fresh liquid-like PRP with no control release mechanisms. One study showed a benefit of PRP to aid in mucosal healing and postextraction socket closure following radiation therapy,[35] while a second study showed no benefit with the use of fresh PRP in decreasing pain or prevention of osteoradionecrosis.[36] Of note, the fresh liquid-like PRP preparations were different between the two studies and both studies were small and possibly underpowered to detect a treatment difference.

Limited data exists on the use of PRP for the treatment of CRI. Iervolino et al. reported on the use of autologous platelet gel in the treatment of chronic Common Terminology Criteria for Adverse Events grade 3–4 cutaneous radiation dermatitis in patients with extremity sarcoma treated with postoperative radiation therapy.[37] Of the 10 patients enrolled on the study, 7 patients had complete re-epithelialization of their ulcerations after a median of 5 platelet gel applications. In the remaining 3 patients, 2 developed progressive or metastatic disease and 1 patient had a partial response to treatment. At a follow-up of 5 years, 6 of the 7 healed patients were alive and free of disease or recurrent cutaneous ulceration. PRP has also been used topically to treat mucosal ulcerations. A case report has been published documenting the successful use of a PRP-based mucoadhesive compound for the treatment of postradiation proctitis following external beam radiation therapy followed by brachytherapy for a uterine carcinoma.[38] While these case studies and small prospective series are encouraging, a large prospective study has yet to be performed which demonstrates the effectiveness of PRP-based products for the treatment of radiation injury. In addition, there are inherent limitations to the use of cell and PRP-based therapies for the treatment of CRI. Biologic therapies are expensive to produce. In the case of PRP-based therapies, inherent variability due to donor differences and preparation protocols make quality control quite challenging. Furthermore, these therapies are not off-the-shelf and cannot be stored for long periods of time which eliminates the possibility of stockpiling and immediate deployment in the event of a large-scale nuclear incident.

PBMs have been designed with the intent of overcoming some of the current limitations of growth factor and PRP-based therapies. PBM materials can be manufactured at a relatively low cost compared to other biologic products.[9,10] The material is manufactured from pooled platelet enriched plasma units to limit lot-to-lot variability and can be stock-piled as it is shelf stable at room temperature.[9] Additionally, this plastic-like PBM material is a nonliquid paste formulation that allows the PBM to stay in place for controlled release. In this study, the use of topical PBMs for the treatment of CRI was investigated using a commercially available ointment, Aquaphor, as a delivery vehicle. The dorsal surface of mice was exposed to a single high dose of 35 Gy to simulate an acute radiation exposure. Topical treatment was initiated at and after 24 hours of radiation exposure for a duration of 5 weeks. More complete healing and fewer recurrent ulcerations were observed in the PBM group compared to the vehicle group, representing an improvement in acute toxicity with PBM treatment. However, when evaluating for late toxicity, in particular fibrosis, while the skin thickness in the PBM-treated mice was less than the vehicle group at the 9 and 17 week postirradiation time points indicating less fibrosis, this difference did not reach statistical significance. Further, an evaluation of fibrosis and chronic inflammatory genes did not show

a significant difference in gene expression between the PBM and vehicle groups at the 17 week postirradiation time point.

One hypothesis to explain why an improvement in acute toxicity did not result in an improvement in late toxicity is the presence of pro-fibrotic signaling molecules contained within the PBM. While plasma contains a myriad of signaling molecules and growth factors, two predominant components in plasma and thus also present in PBMs are TGF-β1 and PDGF.[9] TGF-β1 is known to promote fibrosis following radiation exposure and has been the therapeutic target of agents to mitigate fibrosis[17,19] while PDGFs have been implicated in radiation-induced pulmonary fibrosis.[39] While the presence of these factors appears to have promoted the deposition of extracellular matrix and promote wound healing, the balance of pro- and anti-fibrotic factors in the formulation of PBM for this current study was not adequate to reduce fibrosis, which can cause late toxicity particularly if the exposed site is a joint. An optimal formulation with the correct balance of factors may reduce both acute and late toxicity by promoting healing and preventing the formation of fibrosis.

Potential issues have been suggested with the use of PBMs in the treatment of radiation related injuries. The application of PBMs for the treatment of radiation dermatitis in patients with malignancies treated with radiation therapy is of particular concern. For many of the cancers where cutaneous radiation injury is a major issue, tumorigenesis has been associated with growth factor receptor signaling pathways including in head and neck cancer and soft tissue sarcoma.[40,41] As growth factors promote cell proliferation, there are concerns that use of growth factor-containing materials may result in an increased risk of malignancy as demonstrated by the boxed warning on Regranex Gel.[42] Unlike Regranex Gel that consists of addition of a synthetic growth factor, PBM is based on platelet enriched plasma where the growth factors are present at or below physiological levels.

We note several limitations in this study. First, for this initial study, only one concentration of PBM was investigated using a single treatment schedule. It is possible that a different response would be observed by altering either the concentration of the product or by applying the material for a shorter or longer duration after radiation exposure which is the subject of future studies. Second, this study was performed using a simple cutaneous wound healing model. Depending on the nature of the radiation exposure and in the event of an accompanying detonation, additional tissues are likely to be damaged including underlying bone and soft tissue with potential thermal burns. The goal of future studies is to investigate the use of PBMs for treatment of more complex tissue damage including combined thermal and radiation injuries. Finally, it is difficult to compare the results of this study with those of other studies due to variation in irradiation technique. For this study, the skin received 35 Gy in a single exposure using kV beam energy which was verified with dosimetry. For studies using ^{60}Co, the actual skin dose may be lower than anticipated as higher beam energies result in a skin-sparing effect.

In conclusion, PBMs are off-the-shelf, inexpensive biomaterials derived from platelet enriched plasma designed to naturally stimulate repair of damaged tissues. In this study, we demonstrated that PBMs may be used to help stimulate wound healing of cutaneous tissue following an acute exposure to a high dose of radiation. While PBMs were able to

effectively mitigate acute toxicity following cutaneous radiation exposure, they were less effective at mitigating late toxicity including fibrosis. While this is a promising first study for the use of PBMs to treat cutaneous radiation injury, additional work is needed to fully realize the potential of these materials for the treatment of these challenging wounds.

ACKNOWLEDGMENTS

All plasma-based biomaterials for this study were supplied by Carmell Therapeutics. The authors would like to thank James Sommerfield for fabrication of the mouse holder for radiation delivery as well as fabrication of the imaging device.

Source of Funding: The This work was supported in part with the intramural funds from The Department of Radiation Oncology at Arthur G. James Cancer Hospital, Ohio State University Comprehensive Cancer Center.

REFERENCES

1. Bey E, Prat M, Duhamel P, Benderitter M, Brachet M, Trompier F, et al. Emerging therapy for improving wound repair of severe radiation burns using local bone marrow-derived stem cell administrations. Wound Repair Regen 2010; 18: 50–8. [PubMed: 20082681]
2. Wolbarst AB, Wiley AL Jr, Nemhauser JB, Christensen DM, Hendee WR. Medical response to a major radiologic emergency: a primer for medical and public health practitioners. Radiology 2010; 254: 660–77. [PubMed: 20177084]
3. Brenner DJ, Chao NJ, Greenberger JS, Guha C, McBride WH, Swartz HM, et al. Are we ready for a radiological terrorist attack yet? Report from the centers for medical countermeasures against radiation network. Int J Radiat Oncol Biol Phys 2015; 92: 504–5. [PubMed: 26068482]
4. Ang KK, Trotti A, Brown BW, Garden AS, Foote RL, Morrison WH, et al. Randomized trial addressing risk features and time factors of surgery plus radiotherapy in advanced head-and-neck cancer. Int J Radiat Oncol Biol Phys 2001; 51: 571–8. [PubMed: 11597795]
5. Yamoah K, Showalter TN, Ohri N. Radiation therapy intensification for solid tumors: a systematic review of randomized trials. Int J Radiat Oncol Biol Phys 2015; 93: 737–45. [PubMed: 26530740]
6. Nieder C, Langendijk JA, Guckenberger M, Grosu AL. Prospective randomized clinical studies involving reirradiation: lessons learned. Strahlenther Onkol 2016; 192: 679–86. [PubMed: 27534408]
7. Min CH, Paganetti H, Winey BA, Adams J, MacDonald SM, Tarbell NJ, et al. Evaluation of permanent alopecia in pediatric medulloblastoma patients treated with proton radiation. Radiat Oncol 2014; 9: 220. [PubMed: 25403752]
8. Ryan JL. Ionizing radiation: the good, the bad, and the ugly. J Invest Dermatol 2012; 132: 985–93. [PubMed: 22217743]
9. Smith JD, Weiss LE, Burgess JE, West AI, Campbell PG. Bio-logically active blood plasma-based biomaterials as a new paradigm for tissue repair therapies. Disrupt Sci Technol 2012; 1: 1–11.
10. Schwartzman D, Pasculle AW, Ceceris KD, Smith JD, Weiss LE, Campbell PG. An off-the-shelf plasma-based material to prevent pacemaker pocket infection. Biomaterials 2015; 60: 1–8. [PubMed: 25965281]
11. Hadad I, Johnstone BH, Brabham JG, Blanton MW, Rogers PI, Fellers C, et al. Development of a porcine delayed wound-healing model and its use in testing a novel cell-based therapy. Int J Radiat Oncol Biol Phys 2010; 78: 888–96. [PubMed: 20708345]
12. Schwartzman D, Badhwar V, Kormos RL, Smith JD, Campbell PG, Weiss LE. A plasma-based, amiodarone-impregnated material decreases susceptibility to atrial fibrillation in a post-cardiac surgery model. Innovations (Phila) 2016; 11: 59–63. [PubMed: 26918312]
13. Lu L, Bondra K, Gupta N, Sommerfeld J, Chronowski C, Leasure J, et al. Using NanoDot dosimetry to study the RS 2000 X-ray biological irradiator. Int J Radiat Biol 2013; 89: 1094–9. [PubMed: 23786571]
14. MATLAB and stat toolbox release. Natick, MA, The Math-works, Inc., 2015.

15. Hartigan JA, Wong MA, Algorithm AS. 136: a K-means clustering Algorithm. J R Stat Soc Ser C Appl Stat 1979; 28: 100–8.
16. Haubner F, Ohmann E, Pohl F, Strutz J, Gassner HG. Wound healing after radiation therapy: review of the literature. Radiat Oncol 2012; 7: 162. [PubMed: 23006548]
17. Dormand EL, Banwell PE, Goodacre TE. Radiotherapy and wound healing. Int Wound J 2005; 2: 112–27. [PubMed: 16722862]
18. Muller K, Meineke V. Radiation-induced alterations in cytokine production by skin cells. Exp Hematol 2007; 35: 96–104.
19. Straub JM, New J, Hamilton CD, Lominska C, Shnayder Y, Thomas SM. Radiation-induced fibrosis: mechanisms and implications for therapy. J Cancer Res Clin Oncol 2015; 141: 1985–94. [PubMed: 25910988]
20. Olascoaga A, Vilar-Compte D, Poitevin-Chacon A, Contreras-Ruiz J. Wound healing in radiated skin: pathophysiology and treatment options. Int Wound J 2008; 5: 246–57. [PubMed: 18494630]
21. Muller K, Meineke V. Advances in the management of localized radiation injuries. Health Phys 2010; 98: 843–50. [PubMed: 20445392]
22. Dainiak N, Gent RN, Carr Z, Schneider R, Bader J, Buglova E, et al. Literature review and global consensus on management of acute radiation syndrome affecting nonhematopoietic organ systems. Disaster Med Public Health Prep 2011; 5: 183–201. [PubMed: 21986999]
23. Lataillade JJ, Doucet C, Bey E, Carsin H, Huet C, Clairand I, et al. New approach to radiation burn treatment by dosimetry-guided surgery combined with autologous mesenchymal stem cell therapy. Regen Med 2007; 2: 785–94. [PubMed: 17907931]
24. Benderitter M, Gourmelon P, Bey E, Chapel A, Clairand I, Prat M, et al. New emerging concepts in the medical management of local radiation injury. Health Phys 2010; 98: 851–7. [PubMed: 20445393]
25. Francois S, Mouiseddine M, Mathieu N, Semont A, Monti P, Dudoignon N, et al. Human mesenchymal stem cells favour healing of the cutaneous radiation syndrome in a xenogenic transplant model. Ann Hematol 2007; 86: 1–8. [PubMed: 17043780]
26. Horton JA, Hudak KE, Chung EJ, White AO, Scroggins BT, Burkeen JF, et al. Mesenchymal stem cells inhibit cutaneous radiation-induced fibrosis by suppressing chronic inflammation. Stem Cells 2013; 31: 2231–41. [PubMed: 23897677]
27. Mustoe TA, Purdy J, Gramates P, Deuel TF, Thomason A, Pierce GF. Reversal of impaired wound healing in irradiated rats by platelet-derived growth factor-BB. Am J Surg 1989; 158: 345–50. [PubMed: 2508504]
28. Ryu SH, Kim YH, Lee SW, Hong JP. The preventive effect of recombinant human growth factor (rhEGF) on the recurrence of radiodermatitis. J Radiat Res 2010; 51: 511–7. [PubMed: 20657159]
29. Singh VK, Newman VL, Romaine PL, Wise SY, Seed TM. Radiation countermeasure agents: an update (2011–2014). Expert Opin Ther Pat 2014; 24: 1229–55. [PubMed: 25315070]
30. Reisman SA, Lee CY, Meyer CJ, Proksch JW, Sonis ST, Ward KW. Topical application of the synthetic triterpenoid RTA 408 protects mice from radiation-induced dermatitis. Radiat Res 2014; 181: 512–20. [PubMed: 24720753]
31. Costa DA, Costa TP, Netto EC, Joaquim N, Ventura I, Pratas AC, et al. New perspectives on the conservative management of osteoradionecrosis of the mandible: a literature review. Head Neck 2016; 38: 1708–16. [PubMed: 27240248]
32. Piccin A, Di Pierro AM, Tagnin M, Russo C, Fustos R, Corvetta D, et al. Healing of a soft tissue wound of the neck and jaw osteoradionecrosis using platelet gel. Regen Med 2016; 11: 459–63. [PubMed: 27346565]
33. Scala M, Gipponi M, Mereu P, Strada P, Corvo R, Muraglia A, et al. Regeneration of mandibular osteoradionecrosis defect with platelet rich plasma gel. In Vivo 2010; 24: 889–93. [PubMed: 21164050]
34. Gallesio G, Del Fabbro M, Pol R, Mortellaro C, Mozzati M. Conservative treatment with plasma rich in growth factors-Endoret for osteoradionecrosis. J Craniofac Surg 2015; 26: 731–6. [PubMed: 25974781]

35. Mozzati M, Gallesio G, Gassino G, Palomba A, Bergamasco L. Can plasma rich in growth factors improve healing in patients who underwent radiotherapy for head and neck cancer? A split-mouth study. J Craniofac Surg 2014; 25: 938–43. [PubMed: 24785750]

36. Batstone MD, Cosson J, Marquart L, Acton C. Platelet rich plasma for the prevention of osteoradionecrosis. A double blinded randomized cross over controlled trial. Int J Oral Maxillofac Surg 2012; 41: 2–4. [PubMed: 21782389]

37. Iervolino V, Di Costanzo G, Azzaro R, Diodato AM, Di Macchia CA, Di Meo T, et al. Platelet gel in cutaneous radiation dermatitis. Support Care Cancer 2013; 21: 287–93. [PubMed: 23150187]

38. Perotti C, Del Fante C, Alvisi C, Cervio M. Scudeller L. A cure for post-radiation proctitis? Blood Transfus 2014; 12: s243–4. [PubMed: 23736909]

39. Abdollahi A, Li M, Ping G, Plathow C, Domhan S, Kiessling F, et al. Inhibition of platelet-derived growth factor signaling attenuates pulmonary fibrosis. J Exp Med 2005; 201: 925–35. [PubMed: 15781583]

40. Heldin CH. Targeting the PDGF signaling pathway in tumor treatment. Cell Commun Signal 2013; 11: 97. [PubMed: 24359404]

41. Elferink LA, Resto VA. Receptor-tyrosine-kinase-targeted therapies for head and neck cancer. J Signal Transduct 2011; 2011: 982879. [PubMed: 21776391]

42. Baldo BA. Side effects of cytokines approved for therapy. Drug Saf 2014; 37: 921–43. [PubMed: 25270293]

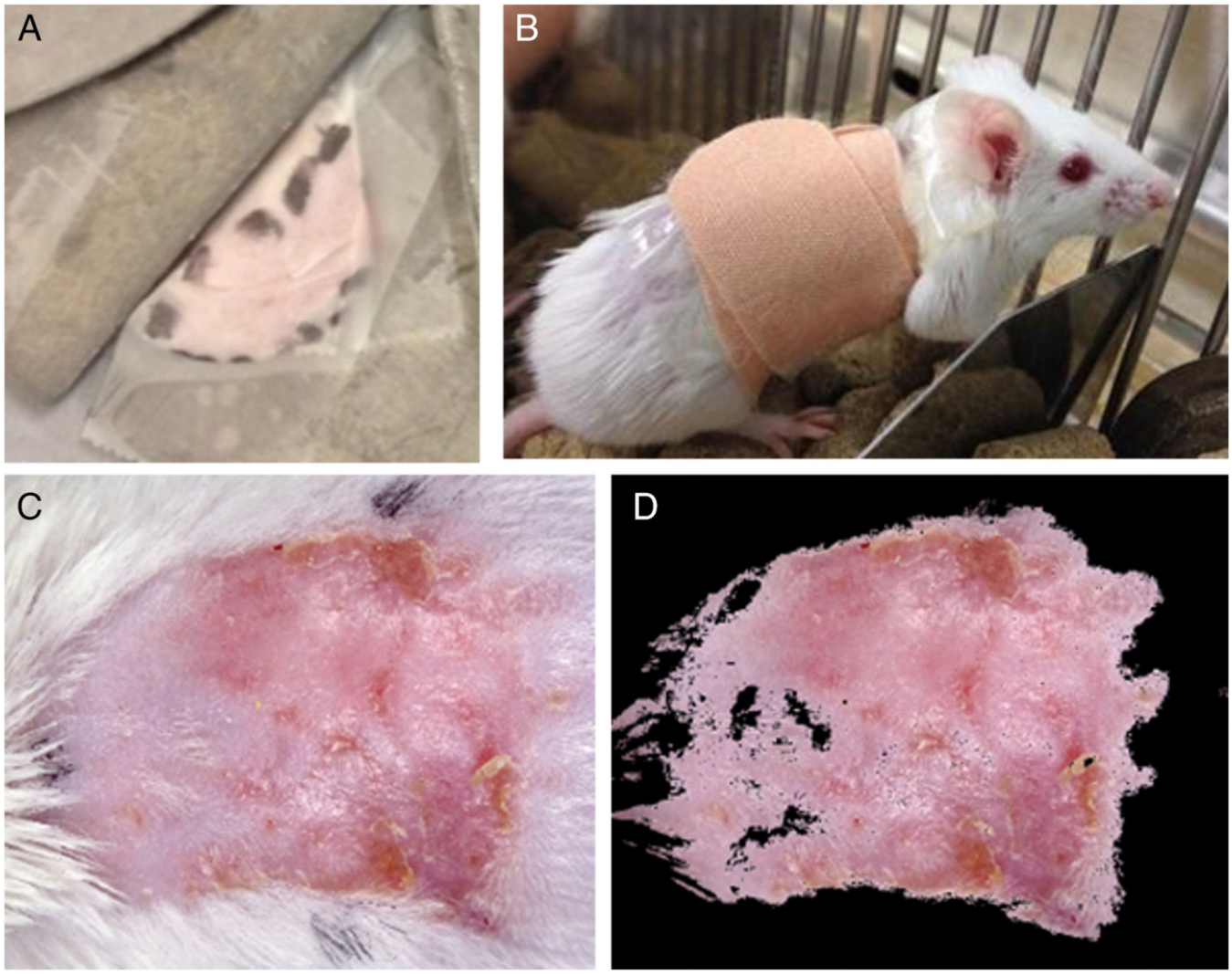

Figure 1.

Radiation exposure, treatment delivery, and quantification of treatment response. (A) The dorsal skin of the mice was pulled through a slit in the lead shielding and taped to the surface of the lead to create a 2 cm diameter localized cutaneous radiation injury (CRI). The irradiated area was outlined with a marker so that the treatment could be applied to the irradiated area prior to the appearance of radiation dermatitis. (B) After application of 0.3 ml of either the treatment or vehicle, the irradiated area was covered with a bandage. (C) Image of a typical CRI at 4 weeks following radiation exposure and treatment with vehicle alone. (D) Same image as shown in (C) following automatic segmentation to quantify wound area.

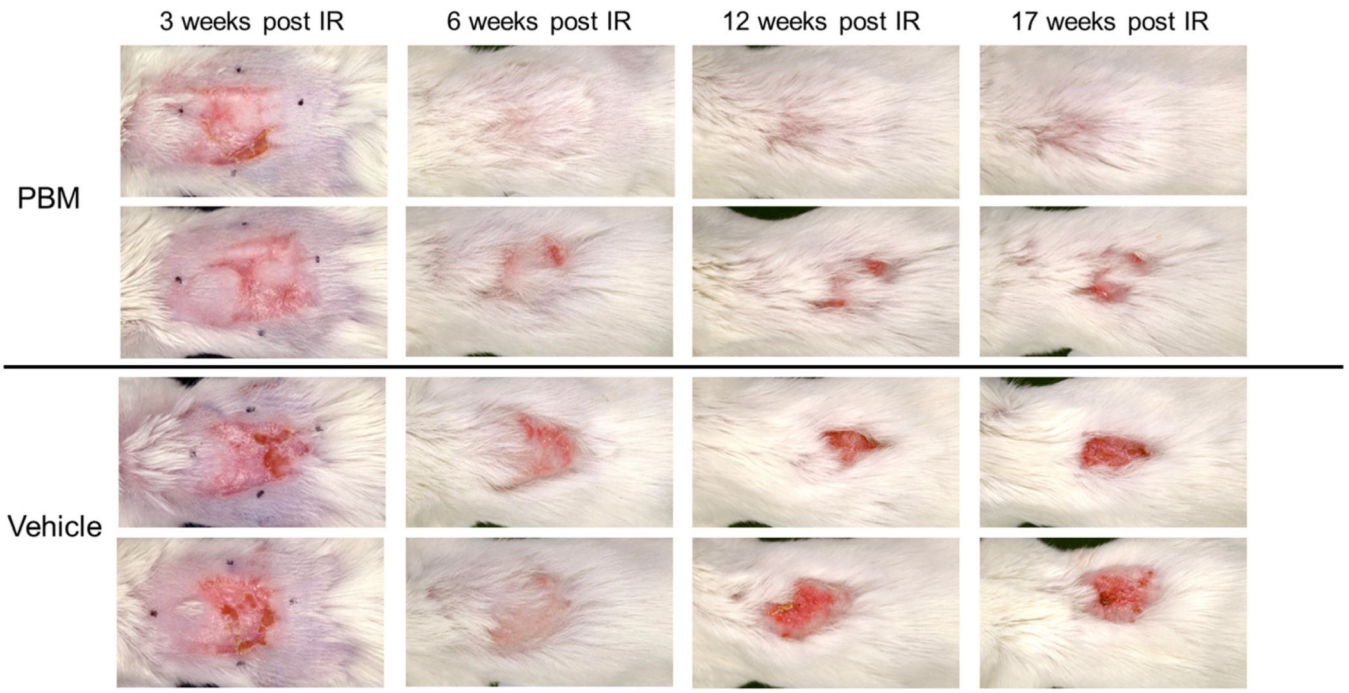

Figure 2.

Serial response of PBM and vehicle-treated mice. The top two rows are examples of mice treated with topical PBM while the bottom two rows are examples of mice treated with vehicle alone. Each column represents a different time point including 3, 6, 12, and 17 weeks after irradiation. More complete healing with fewer recurrent ulcerations were observed in the PBM group compared to the vehicle group. The black marker dots seen at the 3 week time point indicate the area of irradiation on the dorsal surface of the mice.

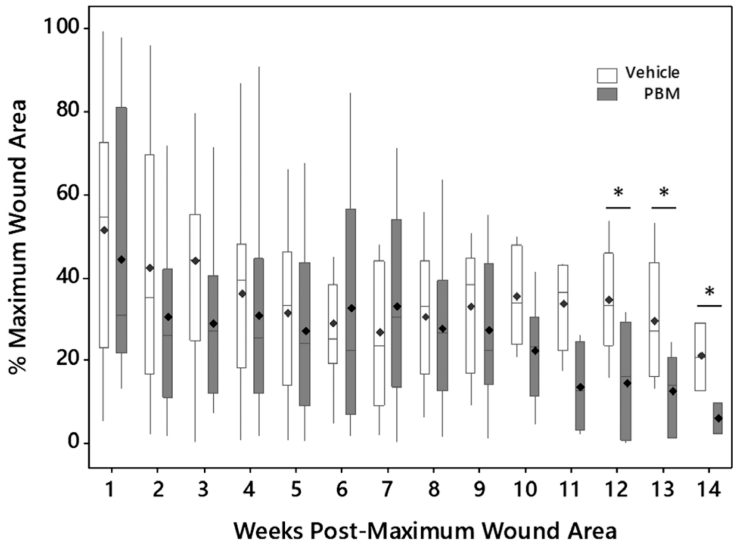

Figure 3.

Wound area closure over time for the mice in the PBM ($n = 22$) and vehicle ($n = 22$) groups. Week 0 (time point not shown) represents the time point of maximum wound area (100%) and is 3–4 weeks after irradiation. The mean value is denoted as ◊. *$p < 0.05$.

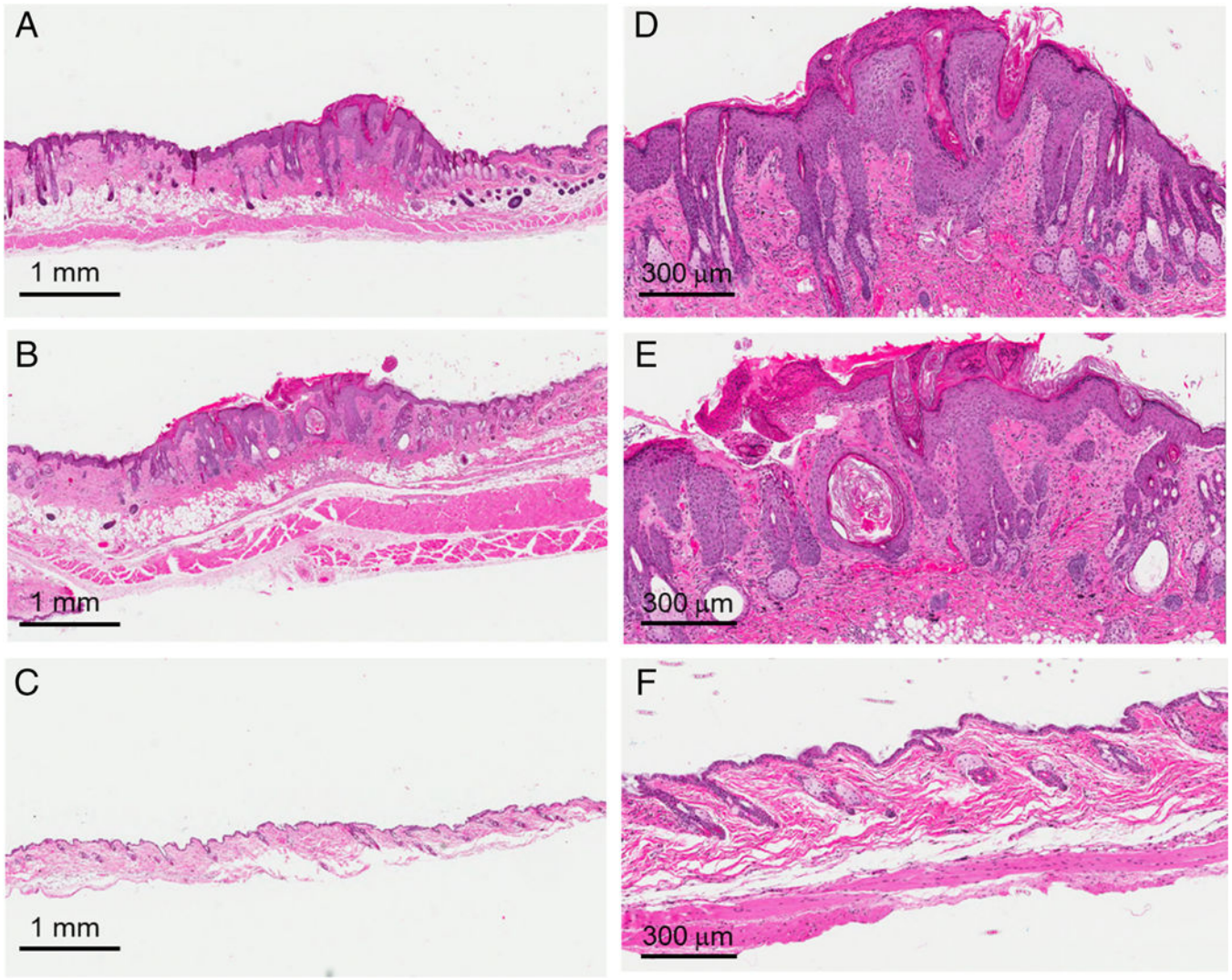

Figure 4.

Skin histology 9 weeks postirradiation. Representative histology from mice after 35 Gy treated with plasma-based biomaterials (PBM) (A,D), vehicle alone (B,E), and control mice without irradiation or treatment (C,F).

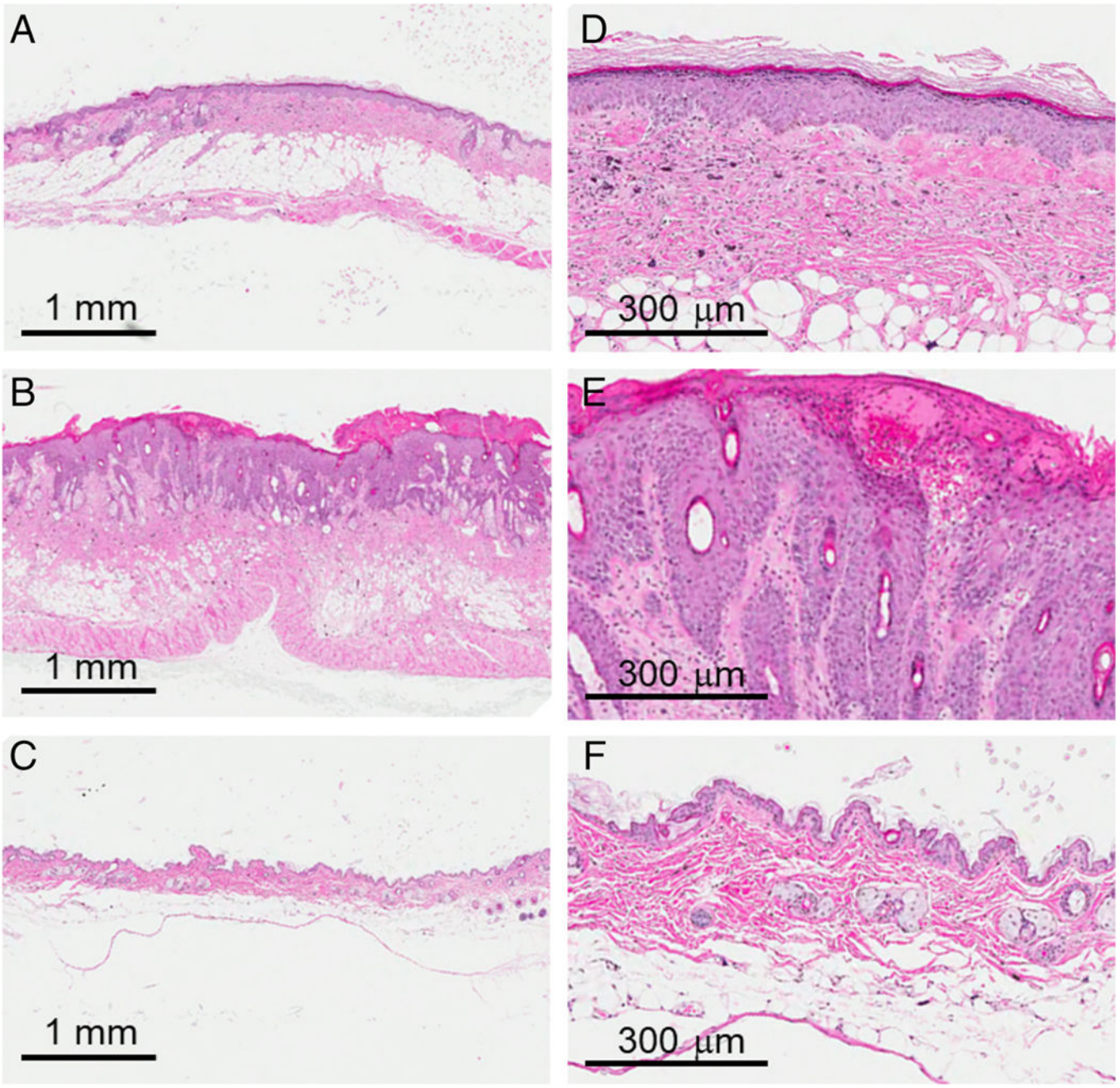

Figure 5.

Skin histology 17 weeks postirradiation. Representative histology from mice after 35 Gy treated with plasma-based biomaterials (PBM) (A,D), vehicle alone (B,E), and control mice without irradiation or treatment (C,F).

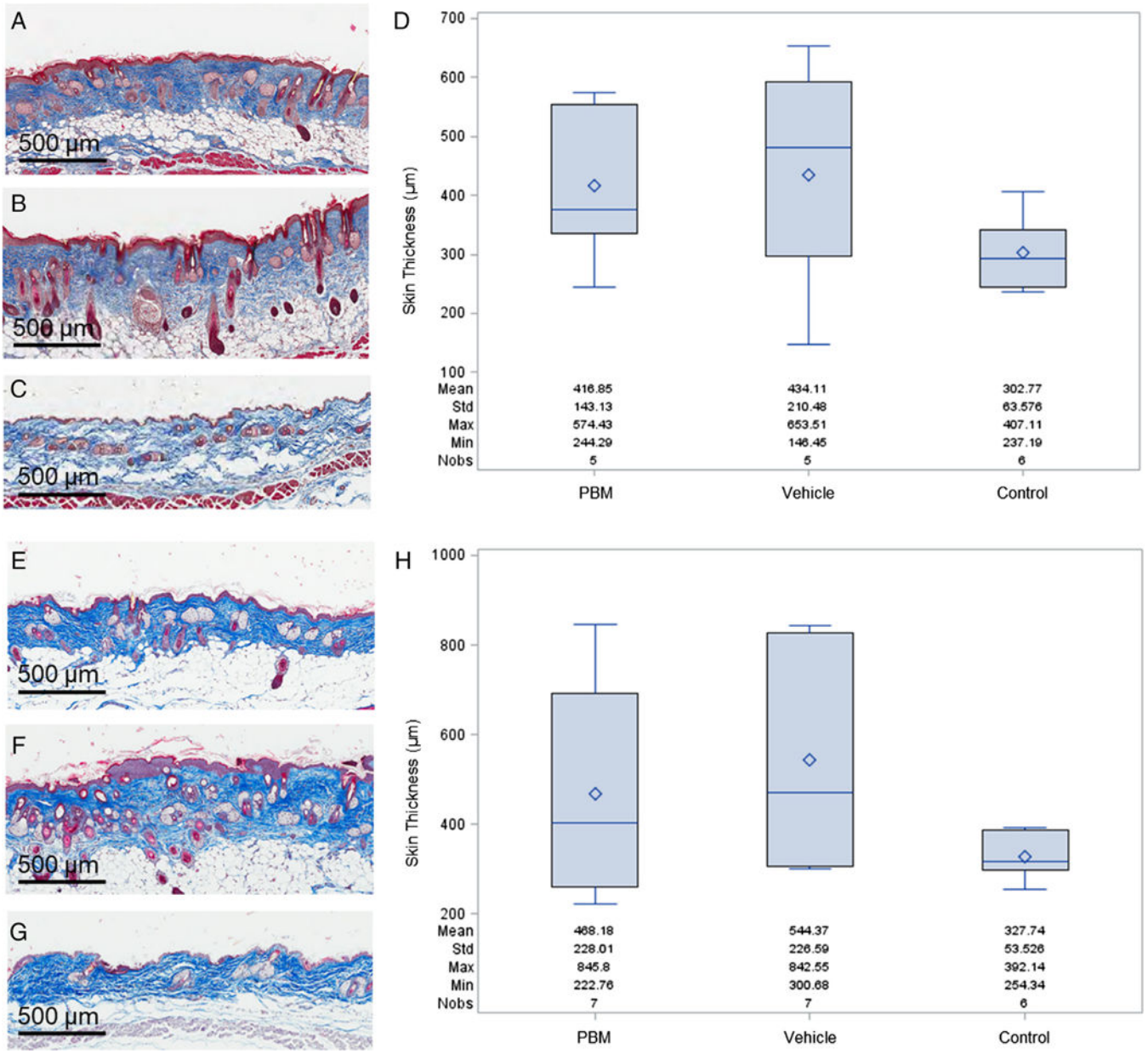

Figure 6.

Skin thickness measurements at 9 and 17 weeks postirradiation. The treated skin was harvested at each of these time points, Masson's trichrome stain was performed, and measurements of skin thickness from the dermal-subcutaneous interface to the external surface of the epidermis were made to measure collagen deposition. Representative images of the 9 week time point are shown in (A) 35 Gy + treatment with plasma-based biomaterial (PBM), (B) 35 Gy + treatment with vehicle alone, (C) control skin without irradiation or treatment. A box plot of the results of the 9 week time point is shown in (D). Representative images of the 17 week time point include (E) 35 Gy + PBM treatment, (F) 35 Gy + vehicle alone, (G) control skin without irradiation or treatment. The box plot for the 17 week time point is shown in (H). The mean value is represented as ◊.

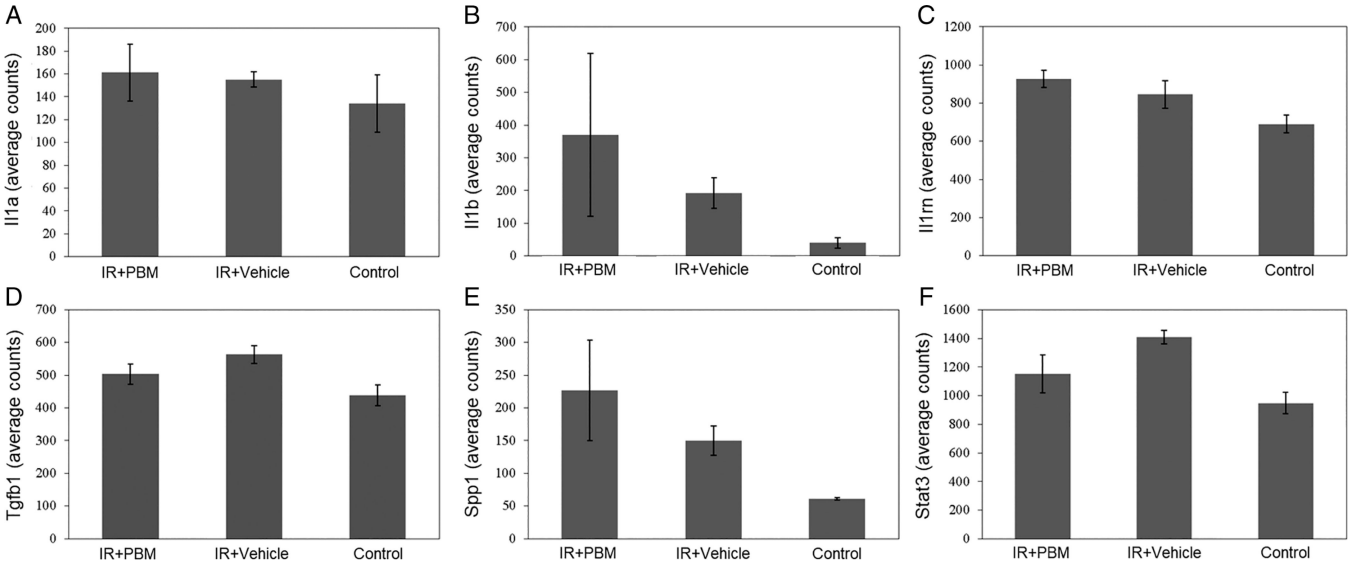

Figure 7.

Chronic inflammatory and fibrosis gene expression analysis. Seventeen weeks postirradiation, the skin was harvested and RNA was extracted from the tissue for analysis. Each bar represents the mean ± SEM from skin samples of five mice.